Supplementary materials

Binding models-tuned room-temperature phosphorescence of the bromo-naphthol derivatives based on cyclodextrins

Ming Liu[a], Chen Zheng[d], Yujing, Zheng[a], Xuan Wu[b,c*], Jianliang Shen[a,b,c*]

[a] *School of Ophthalmology & Optometry, School of Biomedical Engineering, Wenzhou Medical University, Wenzhou, Zhejiang 325035, China*
[b] *Wenzhou Institute, University of Chinese Academy of Sciences, Wenzhou, Zhejiang 325000, China*
[c] *Oujiang Laboratory (Zhejiang Lab for Regenerative Medicine, Vision and Brain Health), Wenzhou, Zhejiang 325001, China*
[d] *College of life and environmental science, Wenzhou University, Wenzhou, Zhejiang 325000, China*

Outline

1. Experimental Procedures

Materials: All reagents and solvents were used as received from commercial suppliers. All aqueous solutions were prepared with distilled water.

Purification and characterization techniques. Flash column chromatography was conducted with 200–300 mesh silica. UV–vis spectra were recorded in a quartz cell (light path = 1 cm) on a CARY5000 spectrophotometer. ^{1}H NMR spectra were recorded on a QUANTUM-I-400 MHz spectrometer. High-resolution mass (HR-MS) spectra were performed on a Q-TOF LC-MS with an ESI mode. Photoluminescence spectra and lifetimes (for solid) were obtained on FSP900 and FSP1000. Quantum efficiency were measured on HAMAMATSU C9920-02.

XRD patterns were obtained at Brucker D8 ADVANCE. FT-IR spectra were recorded on Brucker Tensor II.

2. Synthesis of target molecules

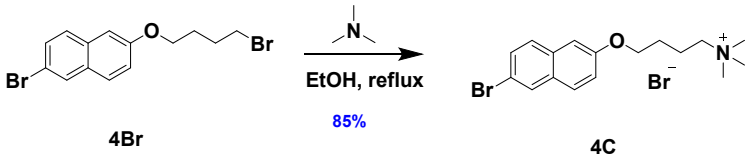

Scheme S1. Synthesis route of compound **4C**.

4C: Compound **4Br**[S1] (1.07 g, 3 mmol) was added to the ethanol solution containing trimethylamine (30 mM, 10 mL), then the mixture was refluxed for 12 h. after being cooled to room temperature, the ethanol was removed under the vacuum, which was washed by diethyl ether. And the targeted molecules were obtained as the white solid (1.06 g, 85% yield). ^{1}H NMR (400 MHz, DMSO-d_6, 298K) δ(ppm): 8.14 (d, J = 1.7 Hz, 1H), 7.86 (d, J = 9.0 Hz, 1H), 7.80 (d, J = 8.8 Hz, 1H), 7.60 (dd, J = 8.7, 2.0 Hz, 1H), 7.39 (d, J = 2.3 Hz, 1H), 7.25 (dd, J = 9.0, 2.5 Hz, 1H), 4.17 (t, J = 5.9 Hz, 2H), 3.45 – 3.38 (m, 2H), 3.09 (s, 9H), 1.97 – 1.88 (m, 2H), 1.84 (dd, J = 12.8, 6.0 Hz, 2H). ^{13}C NMR (101 MHz, DMSO-d_6, 298K) δ(ppm): 157.3, 133.4, 130.2, 129.9, 129. 8, 129.4, 129.1, 120.4, 116.8, 107.3, 67.4, 65.5, 52.8, 26.0, 19.8. For $C_{17}H_{23}BrNO^{+}$ $[M\text{-}Br]^{+}$ 336.0958, found 336.0991.

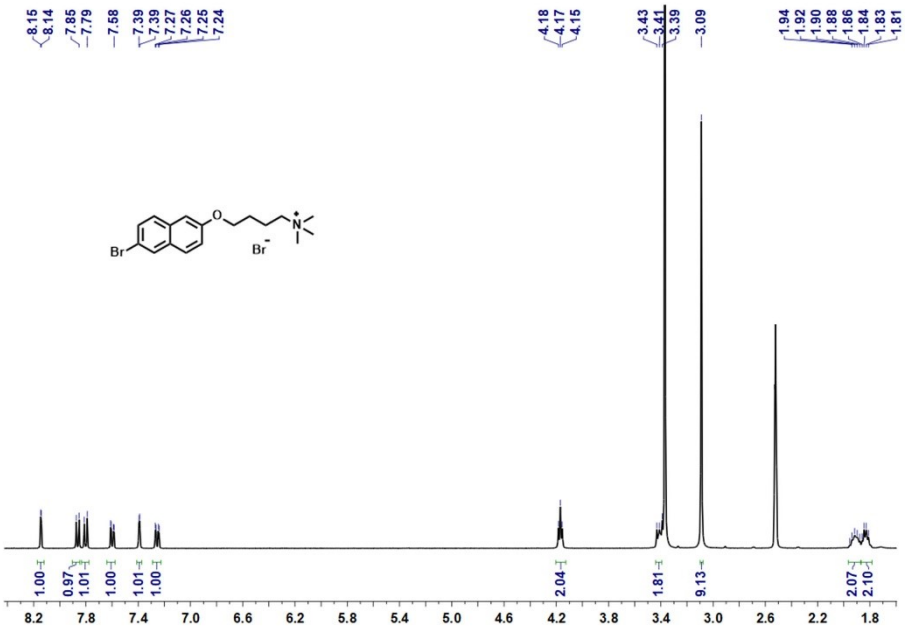

Figure S1. ^{1}H NMR spectrum (400 MHz, DMSO-d_6, 298K) of **4C**.

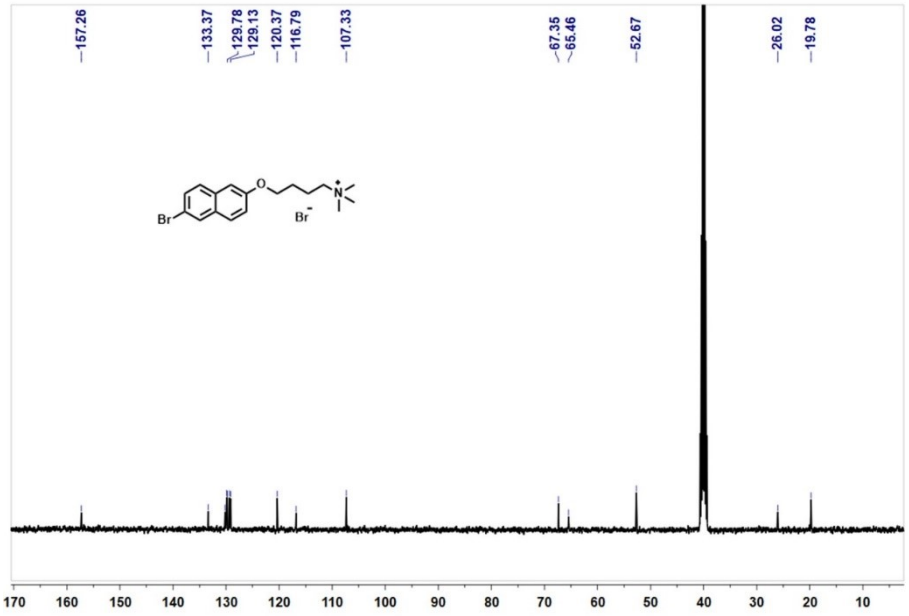

Figure S2. ^{13}C NMR spectrum (101 MHz, DMSO-d_6, 298K) of **4C**.

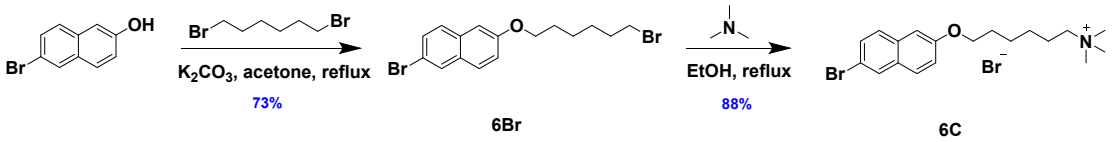

Scheme S2. Synthesis route of compound **6C**.

6Br: K_2CO_3 (4.11 g, 30 mmol) and 1,6-dibromohexane (3.65 g, 15 mmol) were added to a solution of 6-bromo-2-naphthol (1.12 g, 5 mmol) in acetone (50 mL). The resulting mixture was stirred at reflux temperature overnight and the reaction was stopped by filtration and evaporation under vacuum. And the crude product was purified by column chromatography over silica (dichloromethane/*n*-hexane = 1/1, *v/v*) to give the target product **6Br** as a white oil (1.33 g, 73% yield). ^{1}H NMR (400 MHz, $CDCl_3$, 298 K) δ (ppm): 7.90 (d, J = 1.5 Hz, 1H), 7.62 (d, J = 9.0 Hz, 1H), 7.57 (d, J = 8.8 Hz, 1H), 7.49 (dd, J = 8.7, 1.9 Hz, 1H), 7.16 (dd, J = 9.0, 2.4 Hz, 1H), 7.07 (d, J = 2.3 Hz, 1H), 4.03 (t, J = 6.4 Hz, 2H), 3.44 (t, J = 6.8 Hz, 2H), 1.94 – 1.81 (m, 4H), 1.58 – 1.49 (m, 4H). ^{13}C NMR (101 MHz, $CDCl_3$, 298 K) δ (ppm): 157.4, 133.1, 123.0, 129.7, 129.6, 128.5, 128.4, 120.1, 117.0, 106.5, 67.8, 33.9, 32.7, 29.1, 28.0, 25.4.

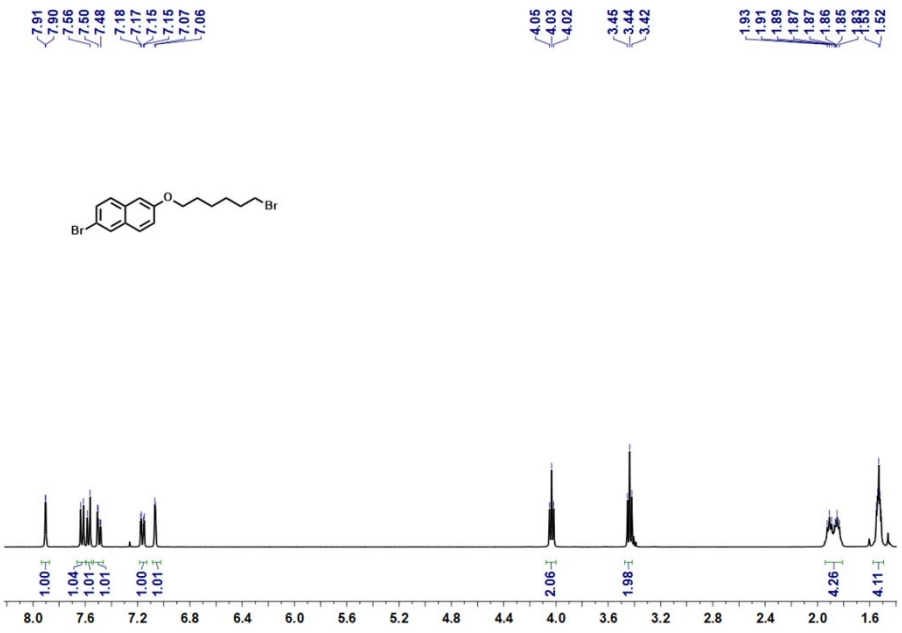

Figure S3. ^{1}H NMR spectrum (400 MHz, D_2O, 298K) of **6Br**.

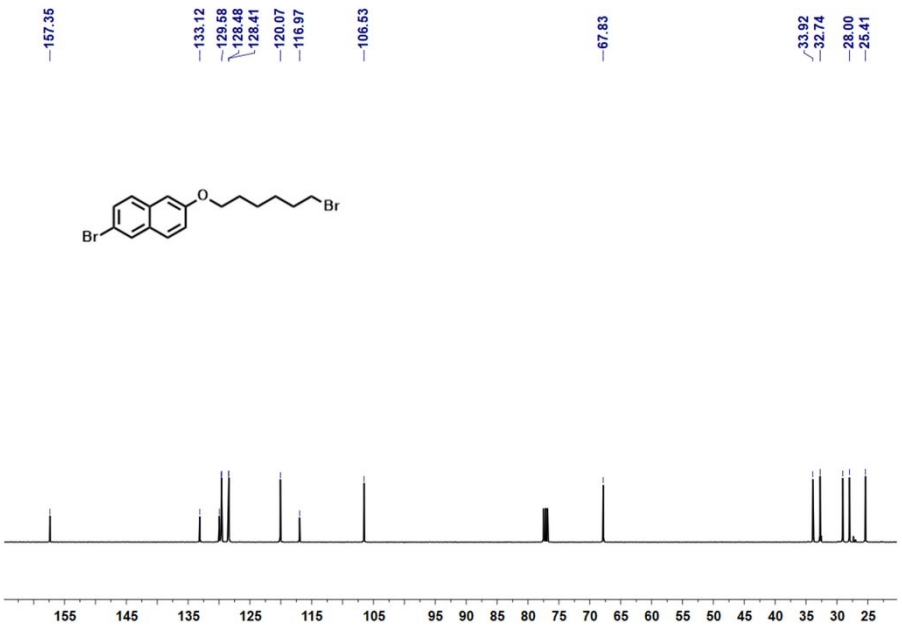

Figure S4. ^{13}C NMR spectrum (101 MHz, DMSO-d_6, 298K) of **6Br**.

6C: Compound **6Br** (1.15 g, 3 mmol) was added to the ethanol solution containing trimethylamine (30 mM, 10 mL), then the mixture was refluxed for 12 h. after being cooled to room temperature, the ethanol was removed under the vacuum, which was washed by diethyl ether. And the targeted molecules were obtained as the white solid (1.17 g, 88% yield). ^{1}H NMR (400 MHz, DMSO-d_6, 298K) δ(ppm): 8.13 (d, J = 1.7 Hz, 1H), 7.84 (d, J = 9.0 Hz, 1H), 7.79 (d, J = 8.8 Hz, 1H), 7.59 (dd, J = 8.8, 2.0 Hz, 1H), 7.37 (d, J = 2.3 Hz, 1H), 7.22 (dd, J = 9.0, 2.5 Hz, 1H), 4.11 (t, J = 6.4 Hz, 2H), 3.35 – 3.24 (m, 2H), 3.06 (s, 9H), 1.89 – 1.79 (m, 2H), 1.79 – 1.67 (m, 2H), 1.59 – 1.48 (m, 2H), 1.44 – 1.33 (m, 2H). ^{13}C NMR (101 MHz, DMSO-d_6, 298K) δ(ppm):157.4, 133.4, 130.1, 129.8, 129.7, 129.4, 129.1, 120.4, 116. 7, 107.2, 67.9, 65.7,

52.6, 28.8, 26.0, 25.6, 22.5. HR-ESI-MS: *m/z* Calcd. For $C_{19}H_{27}BrNO^+$ $[M\text{-}Br]^+$ 364.1271, found 364.1303.

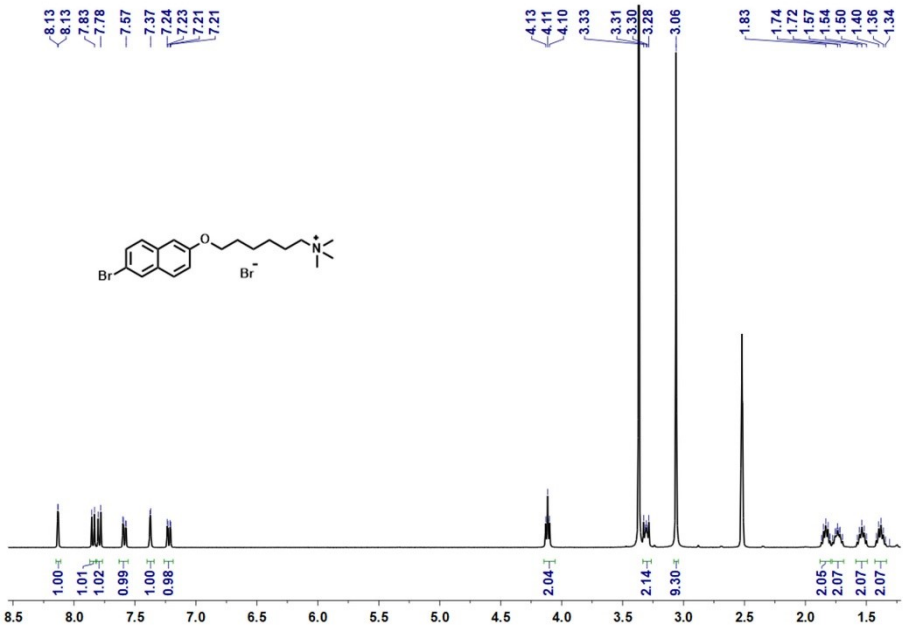

Figure S5. ^{1}H NMR spectrum (400 MHz, DMSO-d_6, 298K) of **6C**.

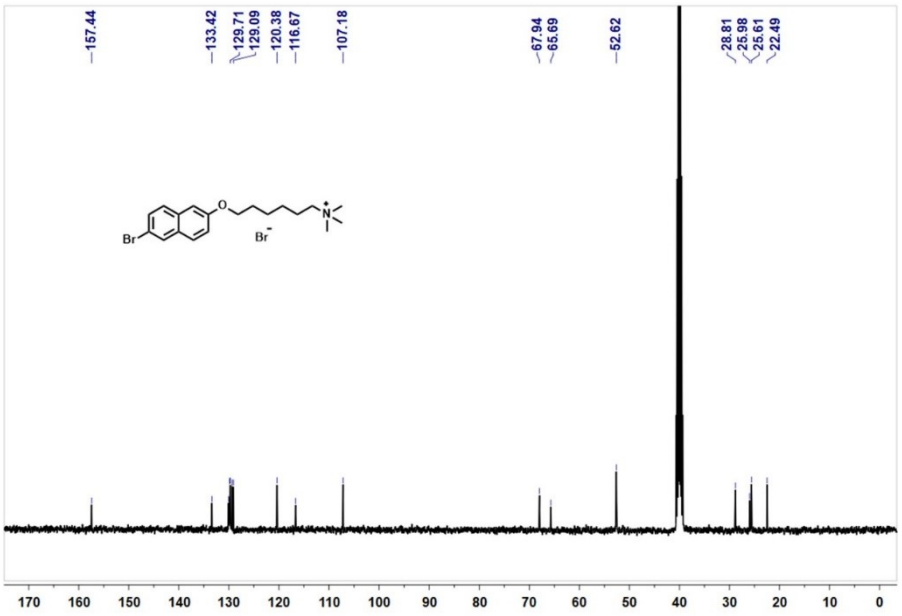

Figure S6. ^{13}C NMR spectrum (101 MHz, DMSO-d_6, 298K) of **6C**.

3. ^{1}H NMR spectra of 6C and cyclodextrins

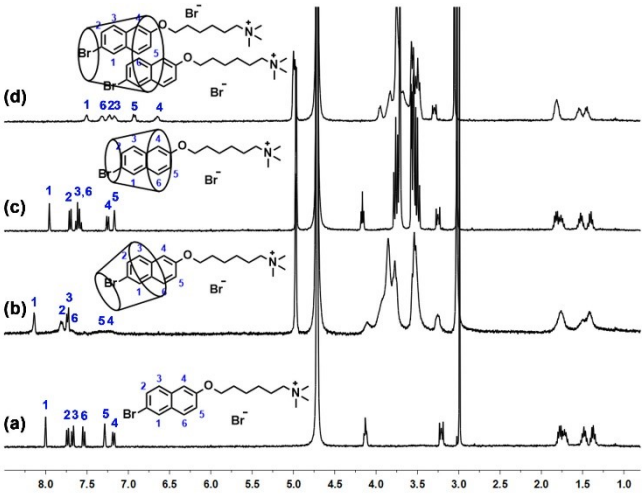

Figure S7. ^{1}H NMR (400 MHz, D_2O, 298 K) spectral changes of **6C** (1) after adding 1.0 equivalent **α-CD** (2), **β-CD** (3) and **γ-CD** (4).

4. 2D NOESY spectra of 4C/6C and cyclodextrins

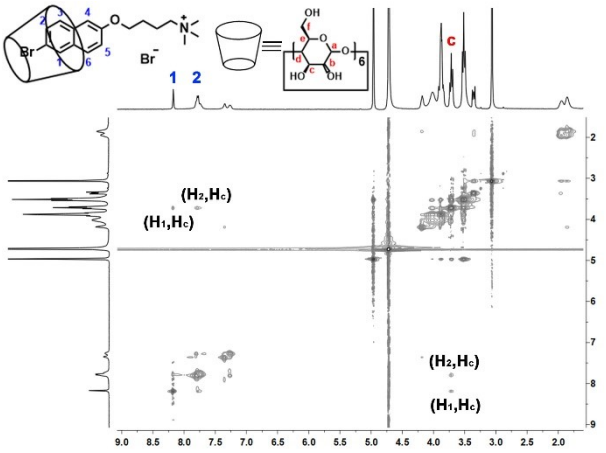

Figure S8. 2D NOESY (400 MHz, D_2O, 298 K) spectrum of **4C⊂α-CD**. ([**4C**] = [**α-CD**] = 2 mM)

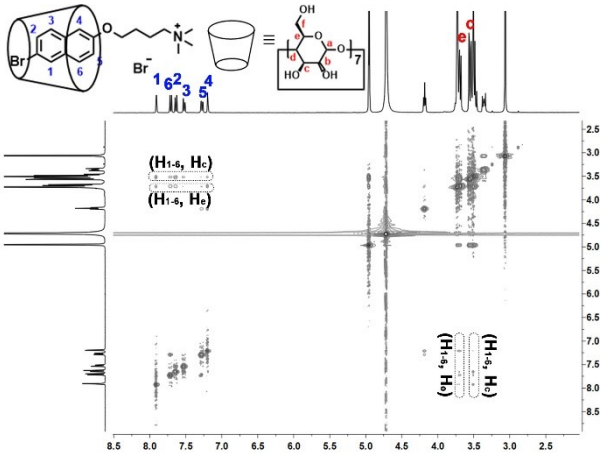

Figure S9. 2D NOESY (400 MHz, D_2O, 298 K) spectrum of **4C⊂β-CD**. ([**4C**] = [**β-CD**] = 2 mM)

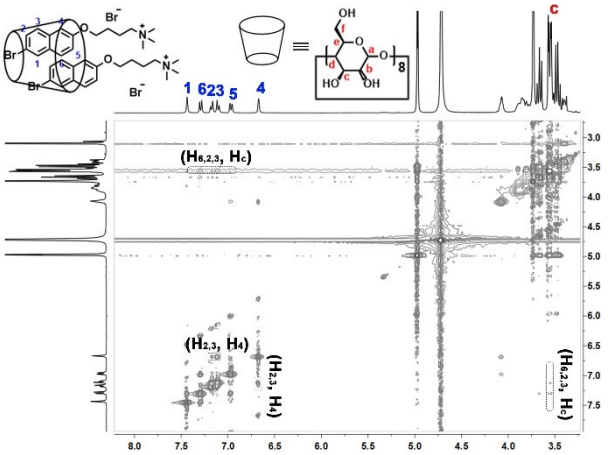

Figure S10. 2D NOESY spectrum (400 MHz, D_2O, 298 K) of **4C⊂γ-CD**. ([**4C**] = [**γ-CD**] = 2 mM)

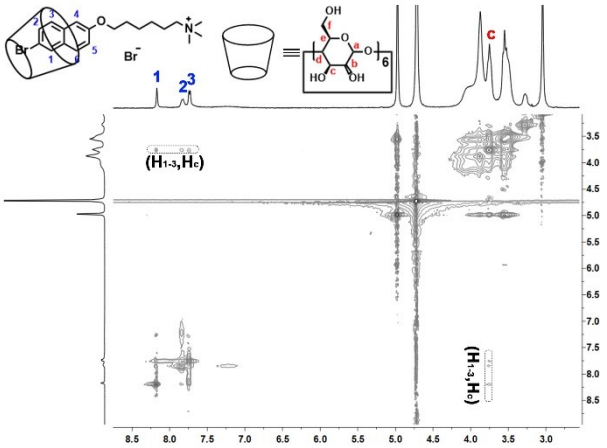

Figure S11. 2D NOESY (400 MHz, D_2O, 298 K) spectrum of **6C⊂α-CD**. ([**6C**] = [**α-CD**] = 2 mM)

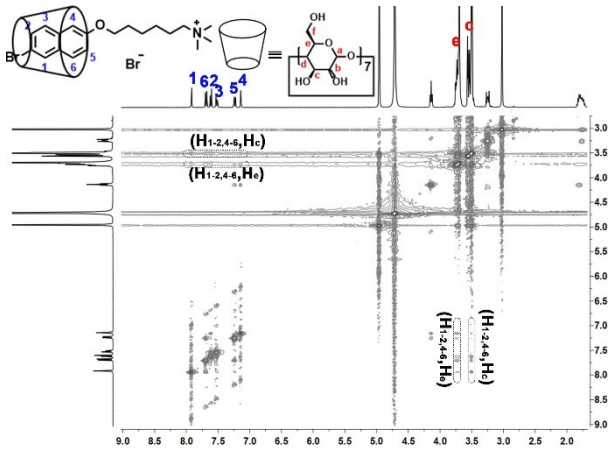

Figure S12. 2D NOESY (400 MHz, D_2O, 298 K) spectrum of **6C⊂β-CD**. ([**6C**] = [**β-CD**] = 2 mM)

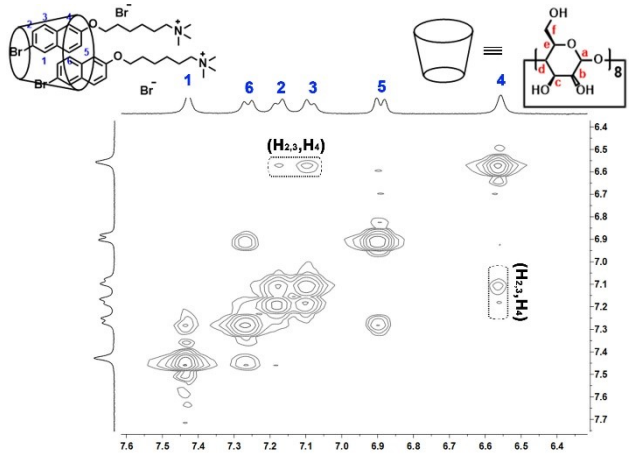

Figure S13. 2D NOESY (400 MHz, D_2O, 298 K) spectrum of **6C⊂γ-CD**. ([**6C**] = [**γ-CD**] = 2 mM)

5. Job's plot of 4C and cyclodextrins

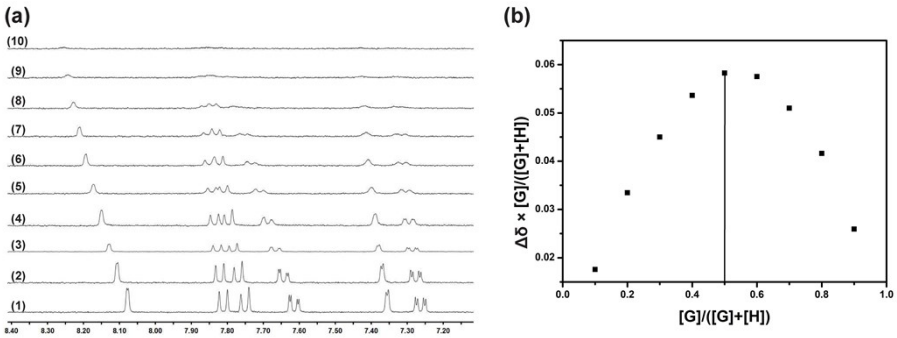

Figure S14. (a) Partial ^1H NMR spectra (400 MHz, D_2O, 298K) of **4C⊂α-CD** complex ([**4C**] + [**α-CD**] = 2 mM) at different ratio in aqueous solution. (1) [**4C**]= 2 mM, (2) [**4C**] = 1.8 mM, [**α-CD**] = 0.2 mM, (3) [**4C**] = 1.6 mM, [**α-CD**] = 0.4 mM, (4) [**4C**]= 1.4 mM, [**α-CD**] = 0.6 mM, (5) [**4C**] = 1.2 mM, [**α-CD**] = 0.8 mM, (6) [**4C**] = 1.0 mM, [**α-CD**] = 1.0 mM, (7) [**4C**] = 0.8 mM, [**α-CD**] = 1.2 mM, (8) [**4C**] = 0.6 mM, [**α-CD**] = 1.4 mM, (9) [**4C**]= 0.4

mM, [**α-CD**] = 1.6 mM, (10) [**4C**] = 0.2 mM, [**α-CD**] = 1.8 mM. (b) Job's plot of **4C** and **α-CD** ([**4C**] + [**α-CD**] = 2 mM).

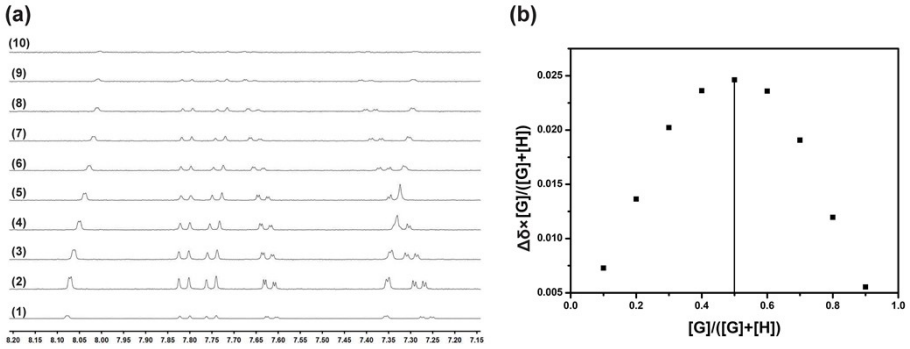

Figure S15. (a) Partial ^{1}H NMR spectra (400 MHz , D_2O, 298K) of **4C⊂β-CD** complex ([**4C**] + [**β-CD**] = 2 mM) at different ratio in aqueous solution. (1) [**4C**] = 2 mM, (2) [**4C**] = 1.8 mM, [**β-CD**] = 0.2 mM, (3) [**4C**] = 1.6 mM, [**β-CD**] = 0.4 mM, (4) [**4C**] = 1.4 mM, [**β-CD**] = 0.6 mM, (5) [**4C**] = 1.2 mM, [**β-CD**] = 0.8 mM, (6) [**4C**] = 1.0 mM, [**β-CD**] = 1.0 mM, (7) [**4C**] = 0.8 mM, [**β-CD**] = 1.2 mM, (8) [**4C**] = 0.6 mM, [**β-CD**] = 1.4 mM, (9) [**4C**] = 0.4 mM, [**β-CD**] = 1.6 mM, (10) [**4C**] = 0.2 mM, [**β-CD**] = 1.8 mM. (b) Job's plot of **4C** and **β-CD** ([**4C**] + [**β-CD**] = 2 mM).

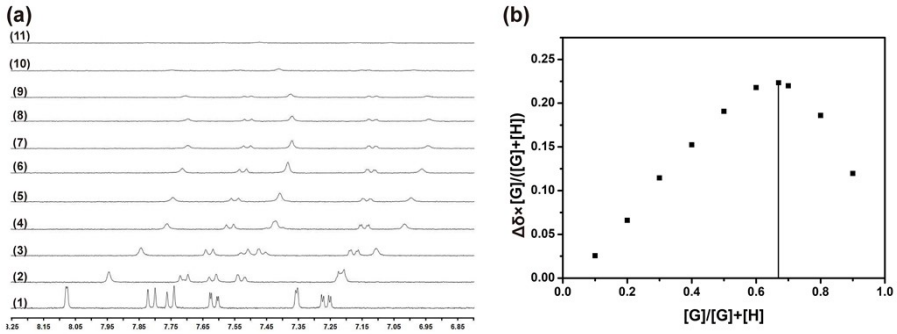

Figure S16. (a) Partial ^{1}H NMR spectra (400 MHz, D_2O, 298K) of **4C⊂γ-CD** complex ([**4C**] + [**γ-CD**] = 2 mM) at different ratio in aqueous solution. (1) [**4C**] = 2 mM, (2) [**4C**] = 1.8 mM, [**γ-CD**] = 0.2 mM, (3) [**4C**] = 1.6 mM, [**γ-CD**] = 0.4 mM, (4) [**4C**] = 1.4 mM, [**γ-CD**] = 0.6 mM, (5) [**4C**] = 1.33 mM, [**γ-CD**] = 0.67 mM, (6) [**4C**] = 1.2 mM, [**γ-CD**] = 0.8 mM, (7) [**4C**] = 1.0 mM, [**γ-CD**] = 1.0 mM, (8) [**4C**] = 0.8 mM, [**γ-CD**] = 1.2 mM, (9) [**4C**] = 0.6 mM, [**γ-CD**] = 1.4 mM, (10) [**4C**] = 0.4 mM, [**γ-CD**] = 1.6 mM, (11) [**4C**] = 0.2 mM, [**γ-CD**] = 1.8 mM. (b) Job's plot of **4C** and **γ-CD** ([**4C**] + [**γ-CD**] = 2mM).

6. Binding constants between 4C and cyclodextrins

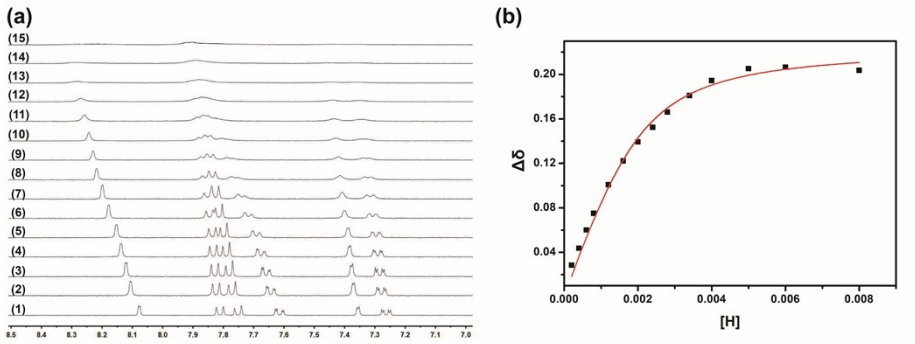

Figure S17. (a) Partial ^{1}H NMR (400 MHz, D_2O, 298K) spectra of **4C** (2 mM) upon addition of **α-CD** (0-8 mM): (1) 0 mM, (2) 0.2 mM, (3) 0.4 mM, (4) 0.6 mM, (5) 0.8 mM, (6) 1 mM, (7) 1.6 mM, (8)2 mM, (9) 2.4 mM, (10) 2.8 mM, (11) 3.4 mM, (12) 4 mM, (13) 5 mM, (14) 6 mM, (15) 8 mM. (b) Nonlinear least-squares analysis of the differential absorbance at 8.1 ppm to calculate the *K*s value[S2].

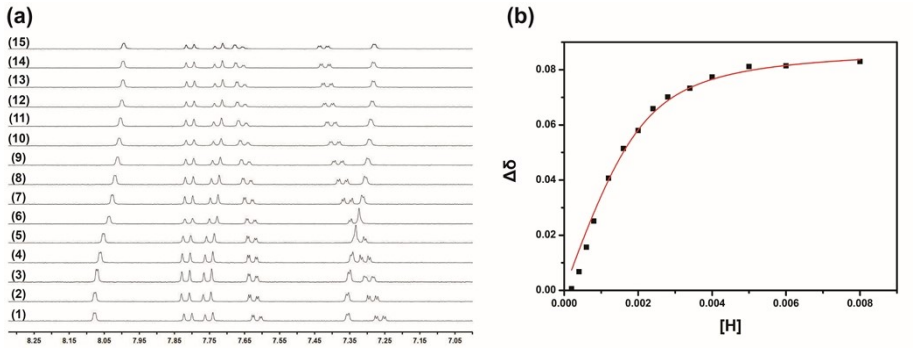

Figure S18. (a) Partial ^{1}H NMR (400 MHz , D_2O, 298K) spectra of **4C** (2 mM) upon addition of **β-CD** (0-8 mM) : (1) 0 mM, (2) 0.2 mM, (3) 0.4 mM, (4) 0.6 mM, (5) 0.8 mM, (6) 1 mM, (7) 1.6 mM, (8)2 mM, (9) 2.4 mM, (10) 2.8 mM, (11) 3.4 mM, (12) 4 mM, (13) 5 mM, (14) 6 mM, (15) 8 mM. (b) Nonlinear least-squares analysis of the differential absorbance at 8.1 ppm to calculate the *K*s value[S2].

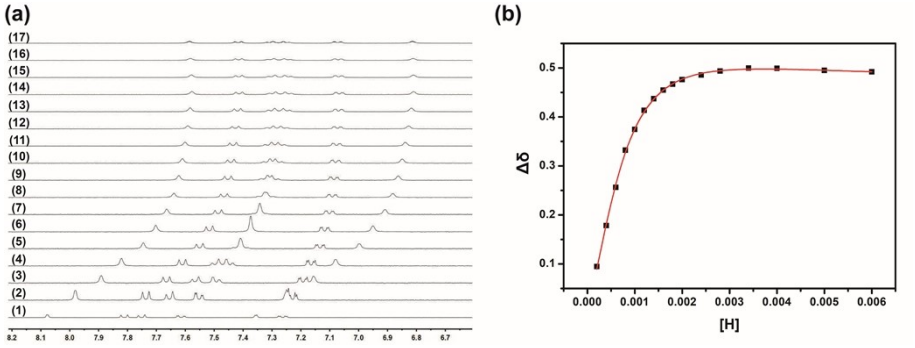

Figure S19. (a) Partial ^{1}H NMR (400 MHz , D_2O, 298K) spectra of **4C** (2 mM) upon addition of **γ-CD** (0-6 mM) : (1) 0 mM, (2) 0.2 mM, (3) 0.4 mM, (4) 0.6 mM, (5) 0.8 mM, (6) 1 mM, (7) 1.2 mM, (8)1.4 mM, (9) 1.6 mM, (10) 1.8 mM, (11) 2 mM, (12) 2.4 mM, (13) 2.8 mM, (14)

3.4 mM, (15) 4 mM, (16) 5 mM, (17) 6 mM. (b) Nonlinear least-squares analysis of the differential absorbance at 8.1 ppm to calculate the *K*s value[S3].

7. UV-Vis spectra between 4C and γ-CD

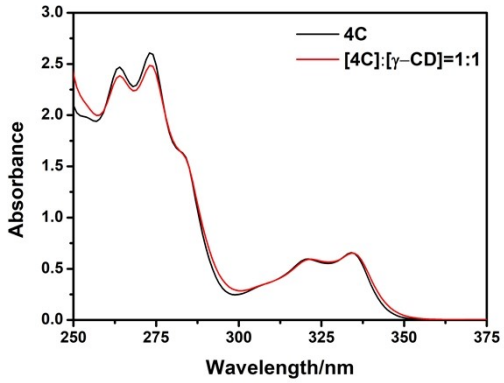

Figure S20. UV/vis spectral changes of **4C** (2 mM) upon adding equivalent **γ-CD**.

8. Fluorescence spectral between 4C and cyclodextrins

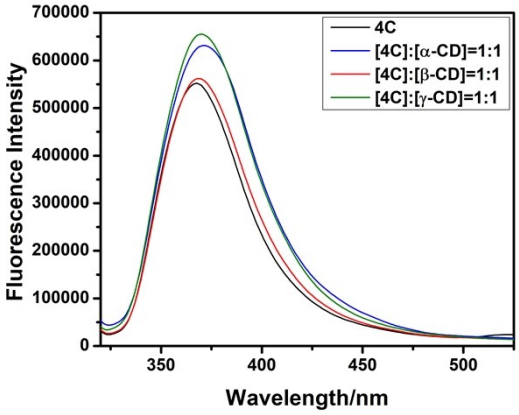

Figure S21. Fluorescence spectral changes of **4C** (1.5×10^{-3} mM) upon adding equivalent **α-CD**、**β-CD** and **γ-CD** in the aqueous solution (Ex: 280 nm, 298 K).

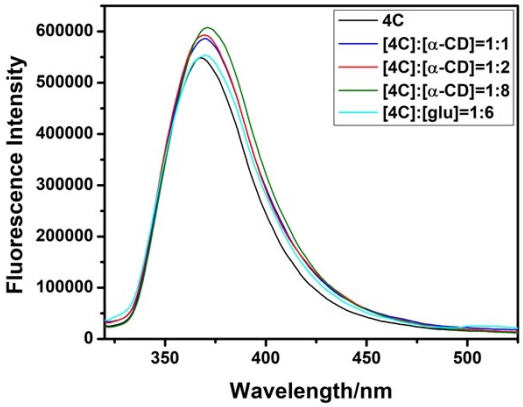

Figure S22. Fluorescence spectral changes of **4C** (1.5×10^{-3} mM), n_{4C}:$n_{\alpha\text{-CD}}$ = 1:1, n_{4C}:$n_{\alpha\text{-CD}}$ = 1:2, n_{4C}:$n_{\alpha\text{-CD}}$ = 1:8, n_{4C}:n_{glu} = 1:6 in the aqueous solution (Ex: 280 nm, 298 K).

9. Excitation spectra in the solid state

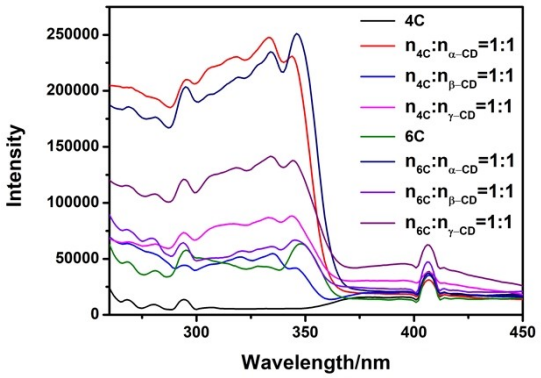

Figure S23. Excitation spectra of **4C**, [**4C**]:[**α-CD**] = 1:1, [**4C**]:[**β-CD**] = 1:1, [**4C**]:[**γ-CD**] = 1:1, **6C**, [**6C**]:[**α-CD**] = 1:1, [**6C**]:[**β-CD**] = 1:1 and [**6C**]:[**γ-CD**] = 1:1 in solid under air at 500 nm (298 K).

10. Photoluminescence properties in the solid state

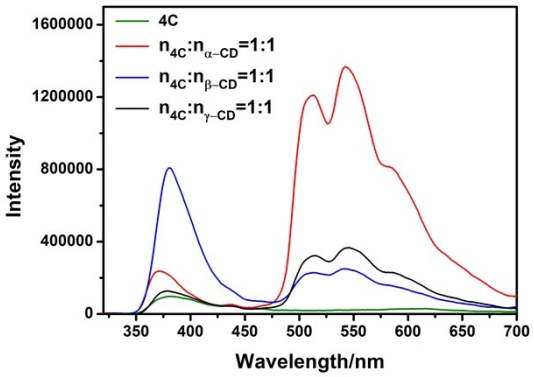

Figure S24. Photoluminescence Spectroscopy of [**4C**], [**4C**]:[**α-CD**] = 1:1, [**4C**]:[**β-CD**] = 1:1 and [**4C**]:[**γ-CD**] = 1:1 in the solid state (Ex: 280 nm, 298 K).

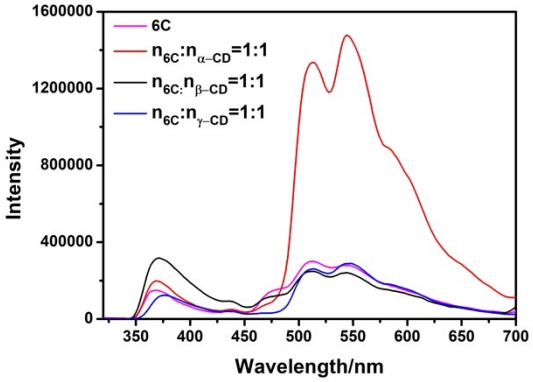

Figure S25. Photoluminescence Spectroscopy of **6C**, [**6C**]:[**α-CD**] = 1:1, [**6C**]:[**β-CD**] = 1:1 and [**6C**]:[**γ-CD**] = 1:1 in the solid state (Ex: 280 nm, 298 K).

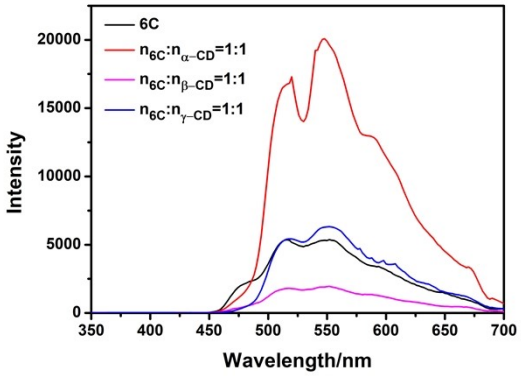

Figure S26. Phosphorescence spectral changes of **6C**, [**6C**]:[**α-CD**] = 1:1, [**6C**]:[**β-CD**] = 1:1 and [**6C**]:[**γ-CD**] = 1:1 in the solid state (Ex: 280 nm, 298 K).

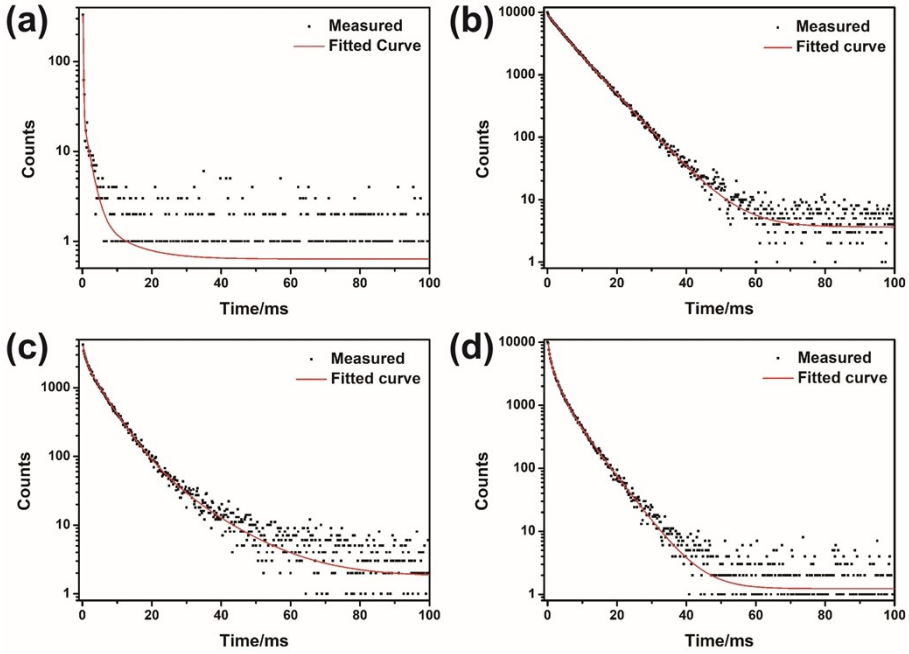

Figure S27. Lifetime at 518 nm **4C** (a), [**4C**]:[**α-CD**] = 1:1 (b), [**4C**]:[**β-CD**] = 1:1 (c), and [**4C**]:[**γ-CD**] = 1:1 (d).

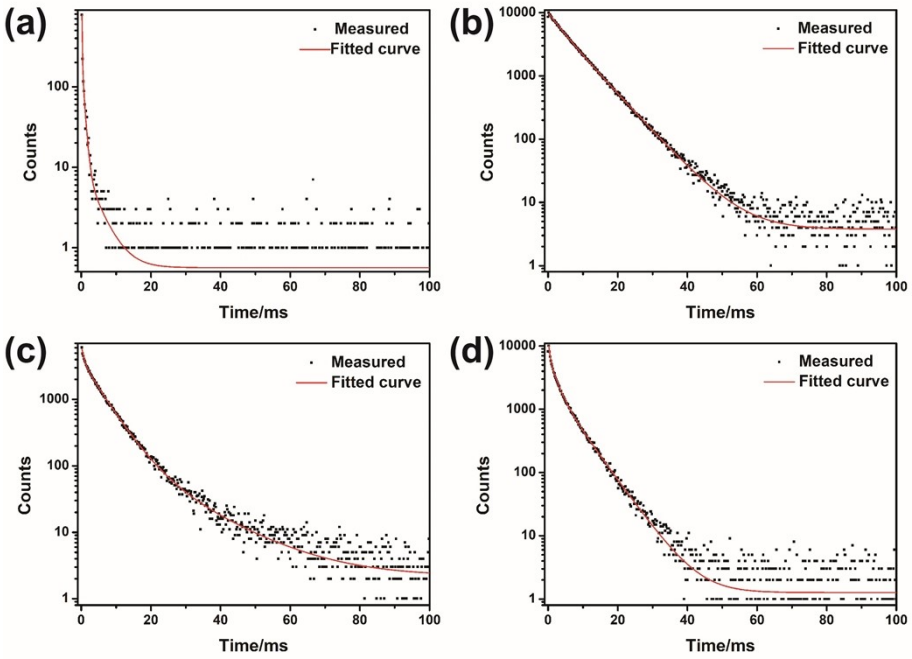

Figure S28. Lifetime at 548 nm **4C** (a), [**4C**]:[**α-CD**] = 1:1(b), [**4C**]:[**β-CD**] = 1:1 (c) and [**4C**]:[**γ-CD**] = 1:1 (d).

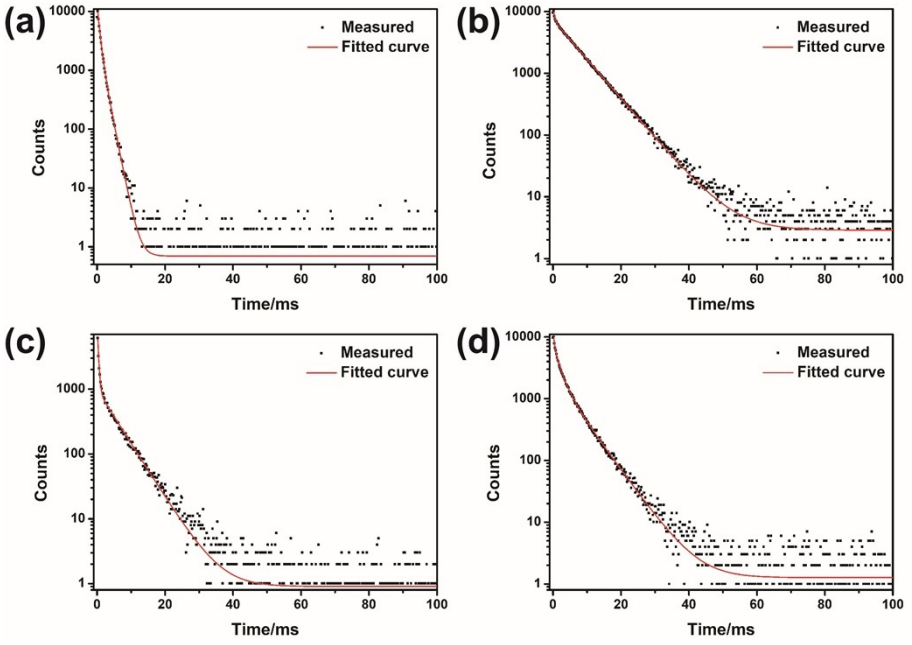

Figure S29. Lifetime at 518 nm **6C** (a), [**6C**]:[**α-CD**] = 1:1 (b), [**6C**]:[**β-CD**] = 1:1 (c) and [**6C**]:[**γ-CD**] = 1:1 (d).

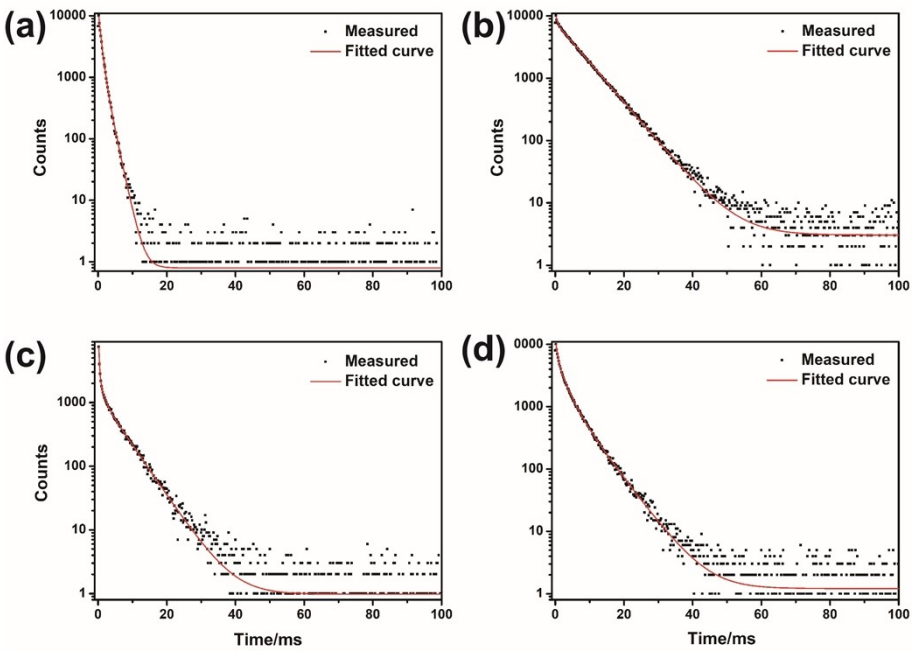

Figure S30. Lifetime at 548 nm **6C** (a), [**6C**]:[**α-CD**] = 1:1 (b), [**6C**]:[**β-CD**] = 1:1 (c) and [**6C**]:[**γ-CD**] = 1:1 (d).

11. Photographs in the solid state

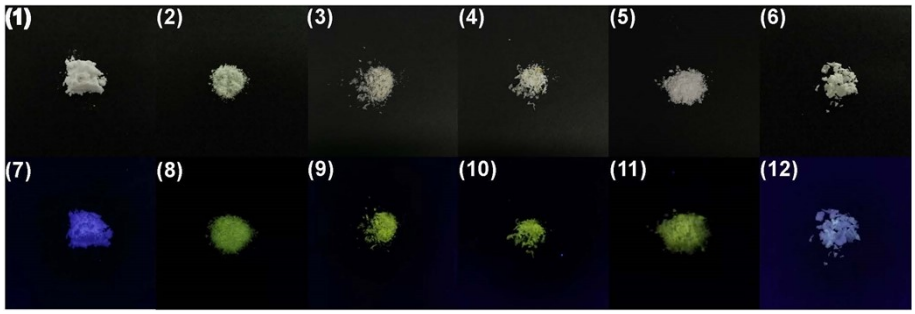

Figure S31. Pictures of **4C** (1, 7), [**4C**]:[**α-CD**] = 1:1 (2, 8), [**4C**]:[**α-CD**] = 1:2 (3, 9), [**4C**]:[**α-CD**] = 1:4 (4, 10), [**4C**]:[**α-CD**] = 1:8 (5, 11) and [**4C**]:[**Glu**] = 1:1 (6, 12) under ambient light (1 - 6) and 365 nm lamp (7 - 12).

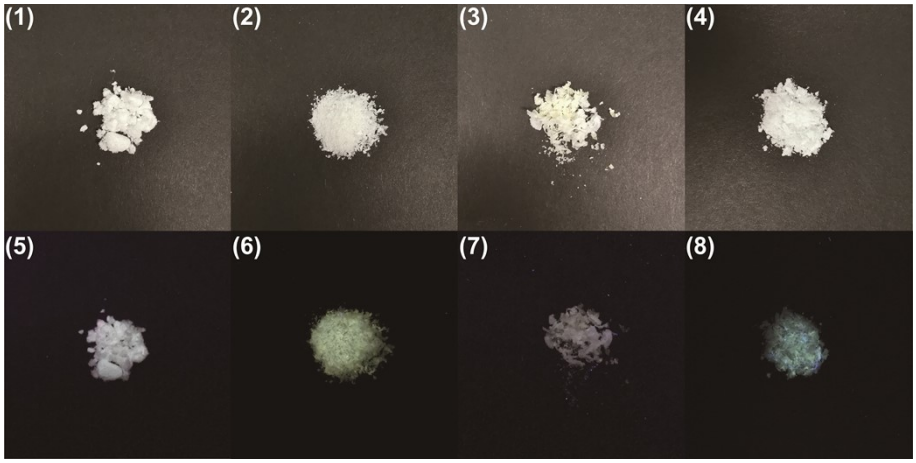

Figure S32. Pictures of **6C** (1, 5), [**6C**]:[**α-CD**] = 1:1 (2, 6), [**6C**]:[**β-CD**] = 1:1 (3, 7) and [**6C**]:[**γ-CD**] = 1:1 (4, 8) under ambient light (1-4) and 365nm lamp (5-8).

Table S1. The photophysical data of **6C** upon adding equivalent **α-CD**, **β-CD** and **γ-CD** in the solid state (Ex: 280 nm, 298 K).

	τ_{Phos} at 548nm/ms	τ_{Phos} at 518nm/ms	τ_{Fluo} at 380nm/ns	Φ_{phos}(%)	Φ_{fluo}(%)
6C	1.07	1.03	1.03	2.34	0.93
[**6C**]:[**α-CD**]=1:1	6.61	6.59	1.20	13.16	0.62
[**6C**]:[**β-CD**]=1:1	3.64	3.44	2.86	3.20	0.78
[**6C**]:[**γ-CD**]=1:1	3.86	3.83	0.88	6.40	0.34

Table S2. The photophysical data of **4C** upon adding different equivalent **α-CD** in the solid state (Ex: 280 nm, 298 K).

	Φ_{phos}(%)
4C	0.56
[**4C**]:[**α-CD**]=1:1	11.47
[**4C**]:[**α-CD**]=1:2	14.20
[**4C**]:[**α-CD**]=1:4	15.35
[**4C**]:[**α-CD**]=1:8	13.38
[**4C**]:[**Glu**]=1:1	20.24

Table S3. The average lifetime at 518 nm in the solid state (Ex: 280 nm, 298 K)**.**

	τ_1 (ms)	Percentage (τ_1)	τ_2 (ms)	Percentage (τ_1)	τ_3 (ms)	Percentage (τ_1)	Average lifetime (ms)
4C	0.01	79.06%	1.75	16.23%	8.95	4.71%	0.71
$\mathbf{n_{4C}:n_{\alpha\text{-}CD} = 1:1}$	3.34	8.91%	7.28	91.09%			6.93
$\mathbf{n_{4C}:n_{\beta\text{-}CD} = 1:1}$	0.65	8.26%	4.87	73.10%	12.83	18.64%	6.01
$\mathbf{n_{4C}:n_{\gamma\text{-}CD} = 1:1}$	0.4	9.83%	2.02	36.72%	5.96	53.45%	3.97
6C	0.62	52.59%	1.49	47.41%			1.03
$\mathbf{n_{6C}:n_{\alpha\text{-}CD} = 1:1}$	0.36	3.39%	6.81	96.61%			6.59
$\mathbf{n_{6C}:n_{\beta\text{-}CD} = 1:1}$	0.32	36.17%	5.22	63.83%			3.45
$\mathbf{n_{6C}:n_{\gamma\text{-}CD} = 1:1}$	0.39	8.82%	1.84	36.47%	5.71	54.71%	3.83

Table S4. The average lifetime at 548 nm in the solid state (Ex: 280 nm, 298 K)**.**

	τ_1 (ms)	Percentage (τ_1)	τ_2 (ms)	Percentage (τ_1)	τ_3 (ms)	Percentage (τ_1)	Average lifetime (ms)
4C	0.1	68.61%	0.64	24.70%	3.86	6.69%	0.48
$\mathbf{n_{4C}:n_{\alpha\text{-}CD} = 1:1}$	3.83	13.44%	7.41	86.56%			6.93
$\mathbf{n_{4C}:n_{\beta\text{-}CD} = 1:1}$	0.67	7.96%	5.03	78.27%	14.79	13.77%	6.03
$\mathbf{n_{4C}:n_{\gamma\text{-}CD} = 1:1}$	0.39	9.44%	1.91	33.46%	5.72	57.10%	3.94
6C	0.69	60.82%	1.67	39.18%			1.07
$\mathbf{n_{6C}:n_{\alpha\text{-}CD} = 1:1}$	0.45	2.78%	6.79	97.22%			6.61
$\mathbf{n_{6C}:n_{\beta\text{-}CD} = 1:1}$	0.2	22.61%	1.02	14.16%	5.47	63.23%	3.65
$\mathbf{n_{6C}:n_{\gamma\text{-}CD} = 1:1}$	0.58	13.88%	2.4	38.59%	6	47.53%	3.86

12. FTIR spectra of 4C and 4C in the presence of α-CD

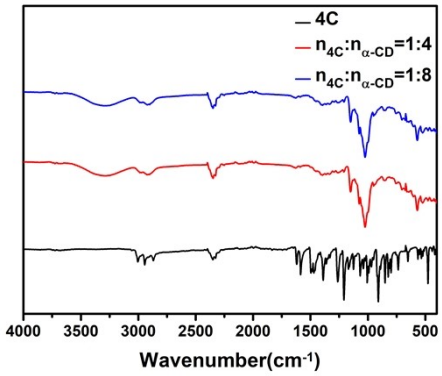

Figure S33. FTIR spectra of **4C** (black line), [**4C**]:[**α-CD**] = 1:4 (red line) and [**4C**]:[**α-CD**] = 1:8 (blue line).

13. XRD profiles of 4C and 4C in the presence of α-CD

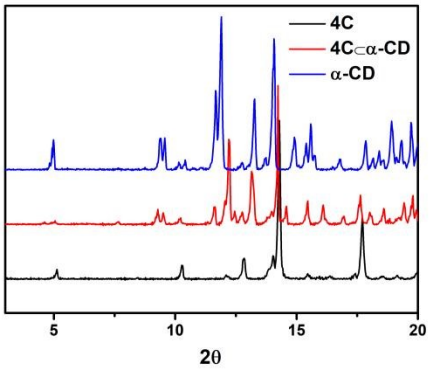

Figure S34. XRD patterns of **4C** (black line), **α-CD** (blue line) and [**4C**]:[**α-CD]** = 1:1 (red line).

14. References

[S1] B. Cherfaoui, T.-K. Guo, H.-P. Sun, W.-L. Cheng, F. Liu, F. Jiang, X.-L. Xu, Q.-D. You, *Bioorg. Med. Chem.* 2016, **24**, 2423-2432.

[S2] X. Wu, Y. Li, C. Lin, X.-Y. Hu, L. Wang, *Chem. Commun.* 2015, **51**, 6832-6835.

[S3] P. Thordarson, *Chem. Soc. Rev.* 2011, **40**, 1305-1323.